

RSC Advances



This is an *Accepted Manuscript*, which has been through the Royal Society of Chemistry peer review process and has been accepted for publication.

Accepted Manuscripts are published online shortly after acceptance, before technical editing, formatting and proof reading. Using this free service, authors can make their results available to the community, in citable form, before we publish the edited article. This *Accepted Manuscript* will be replaced by the edited, formatted and paginated article as soon as this is available.

You can find more information about *Accepted Manuscripts* in the [Information for Authors](#).

Please note that technical editing may introduce minor changes to the text and/or graphics, which may alter content. The journal's standard [Terms & Conditions](#) and the [Ethical guidelines](#) still apply. In no event shall the Royal Society of Chemistry be held responsible for any errors or omissions in this *Accepted Manuscript* or any consequences arising from the use of any information it contains.

Built-in Water Resistance in Organic Transistors Modified with Self-Assembled Monolayers

Cite this: RSC Adv., 2014

Boseok Kang^a, Wi Hyoung Lee^b, Hyun Ho Choi^a, Yeong Don Park^{c,*} and Kilwon Cho^{a,*}

Received 00th January 2014,
Accepted 00th January 2014

DOI: 10.1039/x0xx00000x

www.rsc.org/

We systematically investigated the effects of a self-assembled monolayer (SAM), prepared on the gate dielectric, on the performances of bottom-gate organic field-effect transistor (OFET) devices under various humid environments. OFETs prepared with gate dielectrics modified by depositing a hydrophilic SAM display large variations in their carrier mobilities and on/off ratios when operate under dry or humid conditions. By contrast, the performances of OFETs with a hydrophobic SAM remain relatively constant, regardless of the humidity level. The stability conveyed by the hydrophobic SAM in the presence of humidity is closely related to the water resistance of the SAM, which is based on the hydrophilic and hydrophobic characteristics of the modified gate dielectric.

1. Introduction

Organic semiconductors are quite sensitive to environmental conditions, such as the temperature,¹ pressure,² light,³ and humidity^{4,7}. This susceptibility of OFETs to physical and chemical stimuli has led to the requirement for additional passivation procedures that enhance resistance to these external effects.⁵ Commercial OFET devices must perform reliably under a range of environmental conditions and provide outstanding resistance to those stimuli. Humid conditions, in particular, are a concern for nearly all applications of OFETs.⁸ In the absence of a passivation layer, humid environments unavoidably affect the device performances.⁶ The effects of humidity on OFET device performance have been examined previously,⁴⁻⁷ however further studies are required to reach the goal toward the commercialization of OFETs.

Organic semiconductor thin films are commonly composed of nano- or micro-sized crystalline grains, and numerous grain boundaries are inevitable in the films.⁹⁻¹² Such grain boundaries provide pathways for the diffusion of ambient water molecules into an OFET device.^{4,5} Diffusing water molecules in a semiconductor film can interact with the charge carriers and severely degrade the device performance at humidity levels exceeding some critical value.⁷ Conventional methods for protecting OFETs from humid conditions involve the use of a passivation layer that covers the device^{5,13} and blocks the penetration of water molecules. Since the majority of charge transport in OFETs occurs in the vicinity of the semiconductor/gate dielectric interface,¹⁴ controlling the access of water molecules to this interface offers an efficient approach to improving the environmental stability of OFETs.

In OFETs fabricated with polymer gate dielectrics, the functional groups and polarity of the polymer may be tuned to control the interactions with water molecules, thereby limiting the water that is absorbed into the bulk polymer or adsorbed

onto the surface.^{15,16} The absorbed/adsorbed water molecules within/on the polymeric layer give rise to permanent dipoles that significantly alter the charge-trapping behavior of the OFETs.¹⁶ By contrast, inorganic gate dielectric materials, such as SiO₂, Al₂O₃ and HfO₂, are quite dense and have inter-atomic distances that are shorter than the size of a water molecule.¹⁷ Water molecules, therefore, hardly diffuse into dense bulk dielectrics. Instead, the effects of water molecules are limited to the effects of adsorption onto the inorganic gate dielectric surface. The action of the water molecules is mainly governed by the surface characteristics of the inorganic gate dielectrics, but these effects on OFET performances have not been exhaustively studied.

In an attempt to prevent water adsorption on the surface of the gate dielectric and improve the environmental stability of OFET devices, we applied self-assembled monolayers (SAMs), which modify the surface characteristics of underlying gate dielectric with the simple fabrication procedures.^{18,19} Herein, a set of 5 types of SAMs were tested as SiO₂ surface modifiers to examine, systematically, the effect of adsorbed water molecules on the OFET performances under a variety of operating environments with different humidity levels.

2. Experimental details

2.1 Materials and OFET fabrication

Pentacene field-effect transistors (FETs) were fabricated using a highly doped (p-type) Si wafer as the gate metal and substrate. A thermally grown oxide layer (300 nm thick SiO₂) was employed as the gate dielectric. Prior to treating the SiO₂ layer surface, the wafer dies were cleaned in a piranha solution (70 vol % H₂SO₄ + 30 vol % H₂O₂) for 30 min at 100°C and

washed with distilled water.²⁰ We used 5 coupling agents: aminopropyltriethoxysilane (APS, NH₂), hexamethyldisilazane (HMDS, C1), octyltrichlorosilane (OTS, C8), dodecyltrichlorosilane (DDTS, C12) and octadecyltrichlorosilane (ODTS, C18). All coupling agents except for HMDS were applied using a dipping method in nitrogen filled reactor.^{21,22} Vacuum-dried reaction flasks were charged with anhydrous toluene and the cleaned Si wafers. Solutions of the coupling agent (10 mM) were then added to the flask and left to self-assemble on the wafers for 2 h under nitrogen atmosphere. Self-assembly of the agent molecules take place on the piranha-cleaned SiO₂ surface through the in-situ formation of polysiloxane.¹⁸ The treated wafers were rinsed with toluene and ethanol several times and then baked in an oven at 120°C for 20 min. After baking, the samples were cleaned by ultrasonication in toluene and then rinsed thoroughly with ethanol, followed by vacuum drying prior to film characterization. HMDS was applied by spin-coating the pristine solution onto a UV-ozone-treated SiO₂/Si substrate, followed by baking for 30 min at 150°C.²³ A pentacene layer (50 nm) was deposited onto the modified substrate at a rate of 0.2 Å s⁻¹ at a substrate temperature of 25°C. Device fabrication was completed by evaporating gold through a shadow mask to define source and drain electrodes (100 nm). The channel length and width were 100 and 1000 μm, respectively.

2.2 Characterization

The surface energy of the modified substrates was determined from the contact angles of DI water and diiodomethane droplets on the surface according to the geometric mean equation, $(1 + \cos \theta) \gamma_{pl} = 2(\gamma_s^d \cdot \gamma_{pl}^d)^{1/2} + 2(\gamma_s^p \cdot \gamma_{pl}^p)^{1/2}$, where γ_s and γ_{pl} are the surface energy of the sample and the probe liquid, respectively, and the superscripts d and p refer to the dispersion and polar (nondispersion) components of the surface energy.²⁴ The water contact angles and surface energies of the various SAMs are summarized in Table I. The pentacene morphologies were observed using atomic force microscopy (AFM, Digital Instruments Multimode). Two-dimensional grazing incidence X-ray diffraction (2D GIXD) measurements were performed at the 3C and 9A beamlines at the Pohang Accelerator Laboratory in Korea. The electrical properties of the OFET devices were characterized using a Keithley 4200 semiconductor analyzer at room temperature under a variety of environmental conditions: ambient air (relative humidity of 30%), a vacuum ($\sim 10^{-6}$ Torr), or a nitrogen atmosphere.

3. Results and discussion

Figure 1 shows the device configuration and the chemical structures of the SAM molecules used in this study. SAM molecules can be categorized according to their molecular structures and the surface characteristics of their assembled layers.^{24,25} SAM molecules with a long aliphatic chain are categorized as hydrophobic SAMs. OTS (C8), DDTS (C12), and ODTS (C18) were included in this category. These SAMs showed high water contact angles exceeding 100° due to the hydrophobic nature of the alkyl chains. Hydrophilic SAMs, on the other hand, include polar end functional groups. APS (NH₂) was included in this category and was found to have a low water contact angle of less than 50°. Although HMDS straddled these two categories, this classification system was useful for

explaining the stability of the OFETs under humid environments, which is related to the underlying charge transport mechanisms in the OFETs. For convenience, the piranha-cleaned bare SiO₂ surface (OH) was grouped together with the hydrophilic SAMs in this discussion due to its extremely hydrophilic surface characteristics (with a water contact angle below 10°).

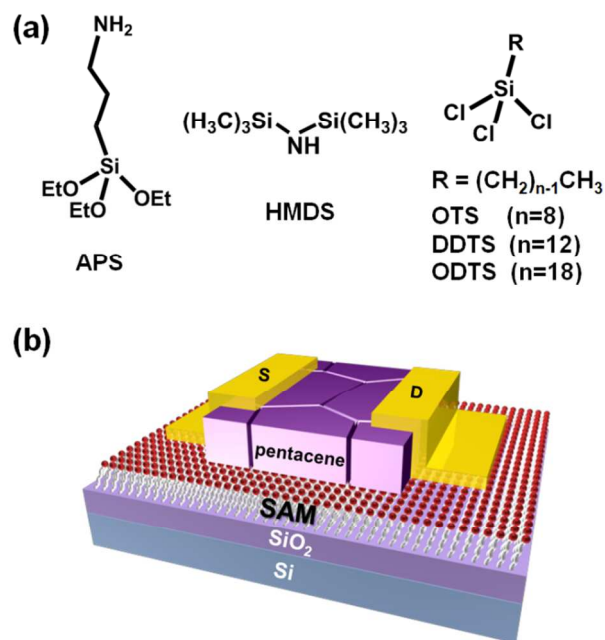


Figure 1. (a) Chemical structures of the materials used in the experiment. (b) The device configuration of the pentacene FETs.

In the case of bottom-gate OFETs, noticeable variation in the device performance under humid conditions would be generated through the following steps: water molecules in ambient air first arrive at the air/semiconductor interface, next diffuse into the bulk of the semiconductor, and finally reach the semiconductor/gate dielectric interface, where majority of charge transport in OFETs take places.^{8,26} Therefore, organic semiconductor films with large grain sizes can be advantageous for stabilizing OFETs against humidity because water molecules can diffuse through the grain boundaries easily.²⁷ Taking this into account, we characterized the morphologies and crystalline structures of the pentacene thin films.

AFM images of the pentacene thin films that formed on the SAMs are shown in Figure 2a. The Stranski–Krastanov growth mode (mixed growth, SK mode) occurred on the substrates with high surface energy.²⁸ In the SK mode, molecules approaching substrate are strongly bound to the substrate and intermolecular interaction is relatively weak, which leads to the formation of a monolayer on the surface. This growth behavior is favored especially in the formation of the first pentacene layer, when surface energy of a substrate is typically higher than that of pentacene (42–48 mJ m⁻²).²⁹ As a result, gate dielectrics with high surface energy, such as bare SiO₂ or APS, yielded relatively large pentacene grain sizes. It should be noted that the charge carrier mobility is not directly related to the size of pentacene grains; the crystallinity, molecular orientation, and interconnectivity within the thin films are also important factors that govern the charge carrier mobility.

Table I. Water contact angles and surface energies of the various SAM-treated SiO₂ gate dielectrics, the grain sizes of the pentacene, and the saturation mobilities (μ) of the corresponding pentacene FETs under ambient air, a vacuum, a nitrogen atmosphere, or ambient air again (air2). *Data were derived from ref 38.

SAMs	Water contact angle (°)	Surface energy (mJ m ⁻²)	Pentacene grain size (μm)	μ^{air} (cm ² V ⁻¹ s ⁻¹)	μ^{vac} (cm ² V ⁻¹ s ⁻¹)	μ^{nitrogen} (cm ² V ⁻¹ s ⁻¹)	μ^{air2} (cm ² V ⁻¹ s ⁻¹)
Bare	~0	287*	0.81	0.06	0.29	0.22	0.10
APS	57	48	0.88	0.03	0.10	0.09	0.07
HMDS	72	44	0.47	0.31	0.74	0.40	0.36
OTS	100	28	0.26	0.49	0.50	0.49	0.49
DDTS	103	27	0.21	0.26	0.22	0.20	0.20
ODTS	105	26	0.15	0.14	0.11	0.11	0.10

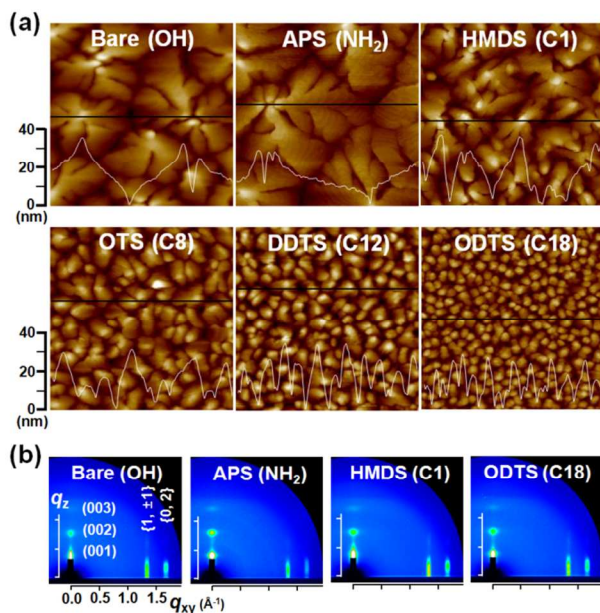


Figure 2. (a) AFM images (2.5 μm × 2.5 μm) and (b) two-dimensional grazing-incidence X-ray diffraction (2D GIXD) patterns obtained from the pentacene films prepared on the SiO₂ gate dielectrics and functionalized with various SAMs: bare SiO₂ (OH), APS (NH₂), HMDS (C1), OTS (C8), DDTS (C14), and ODTS (C18).

Next, 2D GIXD measurements were conducted to confirm the molecular orientations and crystal structures of the pentacene films (10 nm thick, Figure 2b). The 2D GIXD patterns from all samples were similar, indicating that the pentacene molecules on the SAM-treated SiO₂ substrates adopted a standing-up orientation (the patterns obtained from the OTS- and DDTS-treated substrates were similar and are not shown here for brevity). The 2D GIXD patterns displayed intense (00 l) crystal reflections and two in-plane reflections. The two in-plane reflections at a given q_{xy} (>0) could be indexed to {1, ±1} and {0, 2}, respectively.²⁷ Since the pentacene molecular orientations and nanoscale crystal structures that formed on the hydrophilic SAMs were similar to those that formed on the hydrophobic SAMs, the results appeared to indicate that only presence of grain boundaries determine the OFET stability in the presence of humid conditions. It should be noted that our pentacene FETs were fabricated without a passivation layer. Surprisingly, the pentacene FETs prepared with the hydrophobic SAMs, however, yielded nearly invariant device performances under humid conditions, although they presented a high number of

water diffusion pathways (large numbers of grain boundaries). By contrast, the pentacene FETs prepared on the hydrophilic SAMs displayed large variations in performance, depending on the environmental conditions.

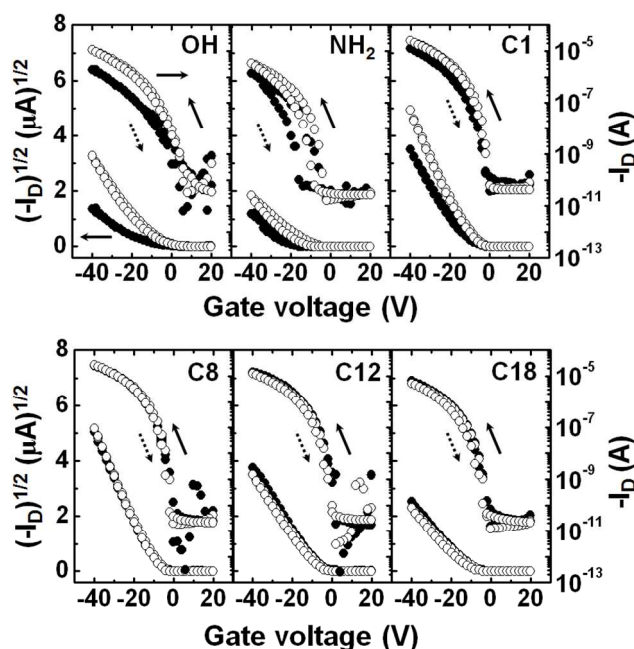


Figure 3. Transfer characteristics (I_D - V_G) of the pentacene FETs ($V_D = -40$ V) prepared with various SAM-treated gate dielectrics under ambient air or under vacuum (● : ambient air, ○ : vacuum).

The device performances were examined in greater detail by measuring the transfer characteristics (I_D and $|I_D|^{1/2}$ vs. V_G at $V_D = -40$ V) of the pentacene FETs in the saturation regime at room temperature under ambient air (relative humidity of 30%) or under vacuum ($\sim 10^{-6}$ Torr). The field-effect mobility (μ) was evaluated in the saturation regime by plotting the square root of the drain current versus gate voltage and fitting the data to the following equation:³⁰ $I_{D,\text{sat}} = (WC_i/2L)\mu(V_G - V_T)^2$, where $C_i = 10.8$ nF cm⁻², $L = 100$ μm, and $W = 1000$ μm. The results obtained from the ambient air and vacuum measurements revealed quite interesting differences between the hydrophilic (bare or APS) or hydrophobic SAMs (OTS, DDTS, and ODTS, Figure 3). The pentacene FETs prepared on the hydrophilic SAMs displayed field-effect mobilities under vacuum (μ^{vac}) that were considerably higher than those measured under air (μ^{air}). By contrast, the field-effect mobilities of devices prepared on

the hydrophobic SAMs remained unchanged under ambient air and vacuum conditions. The average field-effect mobilities obtained from devices prepared using the various SAMs and submitted to various operating conditions are summarized in Figure 4a and Table I.

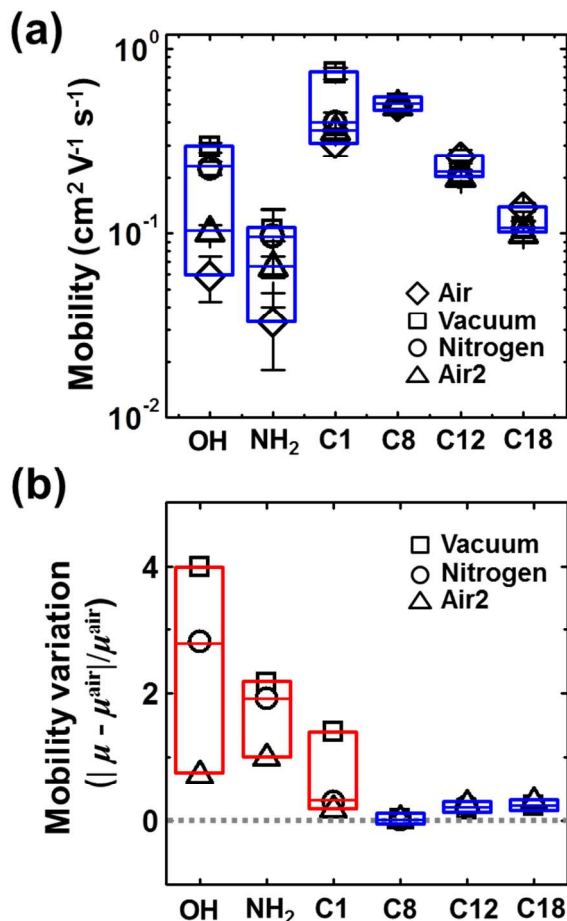


Figure 4. (a) Summary of the field-effect mobilities of the pentacene FETs operated under various environmental conditions (ambient air, vacuum, nitrogen atmosphere, and ambient air again (air2)). (b) Relative changes in the field-effect mobilities (mobility variation, $\Delta\mu = |\mu - \mu^{\text{air}}|/\mu^{\text{air}}$) of FETs prepared with various SAMs, with respect to those measured in air.

The improved mobilities and on-current levels measured under vacuum would arise from the absence of water molecules, rather than from the absence of oxygen. Jurchescu et al. characterized the effects of oxygen and humidity on the performances of OFETs.³¹ Jurchescu's results indicated that oxygen molecules increased hole conduction in pentacene FETs. By contrast, water molecules significantly degraded the transistor performance. The performance degradation in air in this work was also attributed to an increase in the number of adsorbed water molecules near the channel region in the OFETs. Based on the multiple trap and release (MTR) model, the charge carrier mobility depends on the density of shallow trap states.³²⁻³⁴ Therefore, the decrease of conduction in air indicates the increase of shallow trap states in a pentacene layer, which might be induced from the adsorbed water molecules near the channel region. Furthermore, it is noteworthy that the hysteresis of the I_D - V_G curves during the forward and backward sweeps was prominent in the OFET modified with APS. The large

hysteresis measured from the device prepared with APS was attributed to dipole rotation effects. When holes present at the dipoles near the surface of the gate dielectrics, the negative terminal of the dipoles moves toward the holes that produces hysteresis during operation.³⁵ Under humid conditions, water molecules adsorbed onto the APS form dipoles, in addition to the APS molecules themselves. These dipoles can rotate during the gate voltage sweep and provide a large hysteresis. The hysteresis was considerably lower under vacuum conditions, in which the backward I_D - V_G curve was shifted to a much greater degree than the forward curve, most likely due to the presence of fewer dipoles formed by adsorbed water molecules.

Relative variations of field-effect mobility values ($|\mu - \mu^{\text{air}}|/\mu^{\text{air}}$) at various measurement environment compared to those measured at air can be utilized as a quantifying indicator for evaluating environmental stability of OFETs (we defined here $\Delta\mu = |\mu - \mu^{\text{air}}|/\mu^{\text{air}}$). Figure 4b shows the trend of $\Delta\mu$ according to the various SAMs, arranged in order of decreasing surface energy: bare SiO₂ surface > APS > HMDS > OTS > DDTs > ODTS. The values of $\Delta\mu$ measured for OFETs prepared with the high-surface energy SAMs (bare, APS, and HMDS) were largely non-zero. The value of μ^{vac} for an OFET prepared on a bare SiO₂ surface was five times the value of μ^{air} . This result indicated that OFETs modified with the hydrophilic SAMs were quite sensitive to environmental humidity. By contrast, the performances of OFETs prepared with hydrophobic SAMs (OTS, DDTs, and ODTS) remained largely constant under ambient air or under vacuum. These results clarified the effects of the hydrophilic and hydrophobic SAMs. Devices constructed on hydrophobic SAMs displayed minor changes in the carrier mobility under different humidity levels (air or vacuum conditions).

The water resistance properties of the OFETs prepared with various SAMs were further characterized by measuring the performances under nitrogen or ambient air (indicated air2, Figure 4). The devices displayed similar trends in vacuum and in air. The nitrogen gas used in this experiment may include low humidity levels (below 100 PPMv). The OFETs fabricated on the high-surface energy gate dielectrics responded to the small humidity in the nitrogen environment and, thus, showed a slight decrease in mobility compared to the completely dry conditions (vacuum). Furthermore, the value of $\Delta\mu$ for OFETs measured in ambient air ($\Delta\mu^{\text{air2}} = |\mu^{\text{air2}} - \mu^{\text{air}}|/\mu^{\text{air}}$) approached zero, suggesting that differences in the carrier mobility under the various measurement conditions were associated with a reversible process involving the desorption of physisorbed molecules. Furthermore, deviations from zero in the values of $\Delta\mu^{\text{air2}}$ in OFETs prepared with a hydrophilic gate dielectric resulted from the fact that desorbed water molecules within the pentacene films took time to diffuse into the semiconductor-dielectric interface under humid environments. We concluded that the hydrophilic and hydrophobic characteristics of the SAMs contributed to the differences in the water resistance properties of the OFETs.

The water resistance mechanisms that operated at the OFET interfaces are illustrated schematically in Figure 5. Water molecules were more likely to adsorb onto the hydrophilic surfaces due to the strong intermolecular forces between the water molecules and the polar surface.³⁶ Roeselova et al proposed that water readily adsorbs onto a hydrophilic surface by forming hydrogen bonds with the substrate.³⁷ Hydrogen bonding with pre-adsorbed water molecules contributed to the water uptake mechanisms. By contrast, no noticeable water adsorption was observed on the hydrophobic surface. The

hydrophobic surface remained dry up to the point at which water condensation occurred. Water molecules present near the OFET channel region were detrimental to the device performances, and OFETs prepared with hydrophobic gate dielectrics exhibited excellent stability properties under humid conditions. This mechanism explained why the carrier mobilities of pentacene FETs prepared with hydrophilic gate dielectrics decreased under humid conditions, even though they had much fewer grain boundaries to act as diffusion paths for the water molecules.

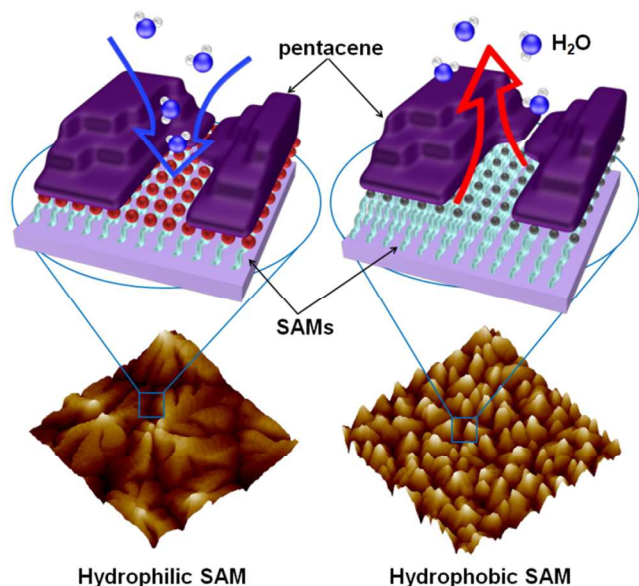


Figure 5. Schematic illustration of the interface-derived water resistance in pentacene FETs prepared with hydrophilic or hydrophobic SAMs.

4. Conclusions

In summary, we systematically investigated the effects of adsorbed water molecules on the performances of pentacene FETs prepared with SAM-modified gate dielectrics. The hydrophilic and hydrophobic characteristics of the SAMs controlled the quantity of water molecules that adsorbed near the OFET channel region. Thus, the field-effect mobility and on-current levels of the OFETs prepared with hydrophilic gate dielectrics improved dramatically under dry conditions. By contrast, the performances of OFETs prepared with hydrophobic SAMs remained constant, regardless of the humidity level. The water resistance properties of the OFET series were attributed to the water resistance of the SAMs prepared on the gate dielectrics.

Acknowledgements

This research was supported by the Center for Advanced Soft Electronics under the Global Frontier Research Program (2011-0031628) of the Ministry of Science, ICT and Future Planning and the Incheon National University Research Grant in 2014. The authors thank the Pohang Accelerator Laboratory for

providing the synchrotron radiation sources at 3C and 9A beam lines used in this study.

Notes and references

^a Department of Chemical Engineering, Pohang University of Science and Technology (POSTECH) and Center for Advanced Soft Electronics (CASE), Pohang 790-784, Korea

^b Department of Organic and Nano System Engineering, Konkuk University, Seoul 143-772, Korea

^c Department of Energy and Chemical Engineering, Incheon National University, Incheon 406-772, Korea

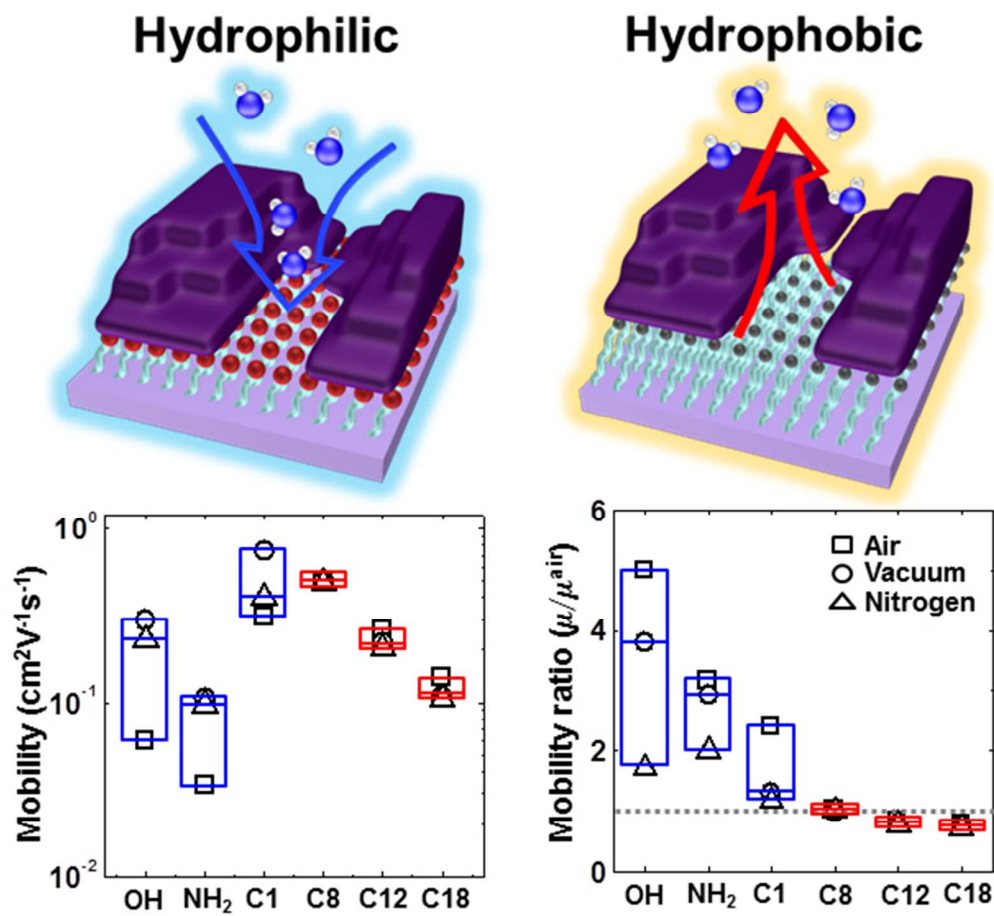
*Corresponding author. Tel: +82-32-835-8679; Fax: +82-32-835-0797.

E-mail address: ydpark@incheon.ac.kr (Y. D. Park), kwcho@postech.ac.kr (K. Cho)

- 1 K. Kuribara, H. Wang, N. Uchiyama, K. Fukuda, T. Yokota, U. Zschieschang, C. Jaye, D. Fischer, H. Klauk, T. Yamamoto, K. Takimiya, M. Ikeda, H. Kuwabara, T. Sekitani, Y. L. Loo and T. Someya, *Nat. Commun.*, 2012, **3**, 723-729.
- 2 Y. Okada, K. Sakai, T. Uemura, Y. Nakazawa and J. Takeya, *Phys. Rev. B*, 2011, **84**, 245308-245312.
- 3 E. Orgiu, N. Crivillers, M. Herder, L. Grubert, M. Patzel, J. Frisch, E. Pavlica, D. T. Duong, G. Bratina, A. Salleo, N. Koch, S. Hecht and P. Samori, *Nat. Chem.*, 2012, **4**, 675-679.
- 4 Z. T. Zhu, J. T. Mason, R. Dieckmann and G. G. Malliaras, *Appl. Phys. Lett.*, 2002, **81**, 4643-4645.
- 5 Y. Qiu, Y. C. Hu, G. F. Dong, L. D. Wang, J. F. Xie and Y. N. Ma, *Appl. Phys. Lett.*, 2003, **83**, 1644-1646.
- 6 Y. D. Park, B. Kang, H. S. Lim, K. Cho, M. S. Kang and J. H. Cho, *ACS Appl. Mater. Interfaces*, 2013, **5**, 8591-8596.
- 7 D. W. Li, E. J. Borkent, R. Nortrup, H. Moon, H. Katz and Z. N. Bao, *Appl. Phys. Lett.*, 2005, **86**, 042105-042107.
- 8 T. Someya, A. Dodabalapur, J. Huang, K. C. See and H. E. Katz, *Adv. Mater.*, 2010, **22**, 3799-3811.
- 9 B. Kang, W. H. Lee and K. Cho, *ACS Appl. Mater. Interfaces*, 2013, **5**, 2302-2315.
- 10 Z. Yu, H. Yan, K. Lu, Y. J. Zhang and Z. X. Wei, *RSC Adv.*, 2012, **2**, 338-343.
- 11 C.-T. Lo, C.-J. Lin, J.-Y. Lee, S.-H. Tung, J.-C. Tsai and W.-C. Chen, *RSC Adv.*, 2014, **4**, 23002-23009.
- 12 C. Pitsalidis, N. Kalfagiannis, N. A. Hastas, P. G. Karagiannidis, C. Kapnopoulos, A. Ioakeimidis and S. Logothetidis, *RSC Adv.*, 2014, **4**, 20804-20813.
- 13 D. K. Hwang, C. Fuentes-Hernandez, J. Kim, W. J. Potscavage, S. J. Kim and B. Kippelen, *Adv. Mater.*, 2011, **23**, 1293-1298.
- 14 G. Horowitz, *Adv. Mater.*, 1998, **10**, 365-377.
- 15 S. H. Kim, H. Yang, S. Y. Yang, K. Hong, D. Choi, C. Yang, D. S. Chung and C. E. Park, *Org. Electron.*, 2008, **9**, 673-677.
- 16 D. K. Hwang, K. Lee, J. H. Kim, S. Im, J. H. Park and E. Kim, *Appl. Phys. Lett.*, 2006, **89**, 093507-093509.
- 17 N. Tohge, K. Tadanaga, H. Sakatani and T. Minami, *J. Mater. Sci. Lett.*, 1996, **15**, 1517-1519.
- 18 A. Ulman, *Chem. Rev.*, 1996, **96**, 1533-1554.
- 19 S. Kobayashi, T. Nishikawa, T. Takenobu, S. Mori, T. Shimoda, T. Mitani, H. Shimotani, N. Yoshimoto, S. Ogawa and Y. Iwasa, *Nat. Mater.*, 2004, **3**, 317-322.

COMMUNICATION

- 20 J. A. Lim, W. H. Lee, D. Kwak and K. Cho, *Langmuir*, 2009, **25**, 5404-5410.
- 21 W. H. Lee, J. Park, Y. Kim, K. S. Kim, B. H. Hong and K. Cho, *Adv. Mater.*, 2011, **23**, 3460-3464.
- 22 D. H. Kim, H. S. Lee, H. Yang, L. Yang and K. Cho, *Adv. Funct. Mater.*, 2008, **18**, 1363-1370.
- 23 B. Kang, H. Min, U. Seo, J. Lee, N. Park, K. Cho and H. S. Lee, *Adv. Mater.*, 2013, **25**, 4117-4122.
- 24 B. Kang, S. Lim, W. H. Lee, S. B. Jo and K. Cho, *Adv. Mater.*, 2013, **25**, 5856-5862.
- 25 H. S. Lee, D. H. Kim, J. H. Cho, M. Hwang, Y. Jang and K. Cho, *J. Am. Chem. Soc.*, 2008, **130**, 10556-10564.
- 26 Y. L. Guo, G. Yu and Y. Q. Liu, *Adv. Mater.*, 2010, **22**, 4427-4447.
- 27 C. R. Kagan, A. Afzali and T. O. Graham, *Appl. Phys. Lett.*, 2005, **86**, 193505-193507.
- 28 R. Ruiz, D. Choudhary, B. Nickel, T. Toccoli, K. C. Chang, A. C. Mayer, P. Clancy, J. M. Blakely, R. L. Headrick, S. Iannotta and G. G. Malliaras, *Chem. Mater.*, 2004, **16**, 4497-4508.
- 29 S. Y. Yang, K. Shin and C. E. Park, *Adv. Funct. Mater.*, 2005, **15**, 1806-1814.
- 30 S. M. Sze, *Semiconductor Device Physics and Technology*, Wiley, 2nd edn., 2001.
- 31 O. D. Jurchescu, J. Baas and T. T. M. Palstra, *Appl. Phys. Lett.*, 2005, **87**, 052102-052104.
- 32 V. Podzorov, E. Menard, A. Borissov, V. Kiryukhin, J. A. Rogers and M. E. Gershenson, *Phys. Rev. Lett.*, 2004, **93**, 086602-086604.
- 33 S. G. J. Mathijssen, M. Cölle, H. Gomes, E. C. P. Smits, B. de Boer, I. McCulloch, P. A. Bobbert and D. M. de Leeuw, *Adv. Mater.*, 2007, **19**, 2785-2789.
- 34 B. Lee, A. Wan, D. Mastrogiovanni, J. E. Anthony, E. Garfunkel and V. Podzorov, *Adv. Mater.*, 2010, **22**, 085302-085305.
- 35 K. Suemori, M. Taniguchi, S. Uemura, M. Yoshida, S. Hoshino, N. Takada, T. Kodzasa and T. Kamata, *Phys. Status Solidi. C*, 2011, **8**, 601-603.
- 36 J. N. Israelachvili, *Intermolecular and surface forces*, Academic press, 2nd edn., 1992.
- 37 M. Szori, P. Jedlovsky and M. Roeselova, *Phys. Chem. Chem. Phys.*, 2010, **12**, 4604-4616.
- 38 A. J. Kinloch, *Adhesion and Adhesives Science and Technology*, Cambridge University Press: Cambridge, U.K., 1987.



161x146mm (96 x 96 DPI)